Thermal Effects on Domain Wall Depinning from a Single Notch

E. Martinez,[1] L. Lopez-Diaz,[2] O. Alejos,[3] L. Torres,[2] and C. Tristan[2]
[1]*Universidad de Burgos, Plaza Misael Banuelos, s/n, E-09001, Burgos, Spain*
[2]*Universidad de Salamanca, Plaza de la Merced s/n, E-37008, Salamanca. Spain*
[3]*Universidad de Valladolid, Prado de la Magdalena, E-47071, Valladolid. Spain*
(Received 7 December 2006; published 27 June 2007)

The statistical behavior of the domain wall depinning from a notch placed in a thin ferromagnetic wire is studied by means of a stochastic one-dimensional model which considers the wall as a rigid object inside a parabolic potential at room temperature. This analysis reveals the key role of thermal fluctuations on the current and field-induced domain wall depinning, and it allows for direct comparison with experiments in order to gain information on the nonadiabaticity degree of the spin torque.

DOI: 10.1103/PhysRevLett.98.267202 PACS numbers: 75.60.Ch, 75.40.Gb, 75.40.Mg, 75.75.+a

Several logic [1] and storage [2] devices have been proposed over the last years based on the domain wall (DW) displacement along thin ferromagnetic wires. The position of the DW can be manipulated by means of a notch [3,4] which acts as the local pinning center for the wall, and the DW depinning can be achieved by means of large enough external magnetic fields H_e and/or in-plane electrical currents j_a [5]. The characterization of the DW depinning process is not only of technological relevance since it determinates the real operability of future devices [6–9]; it is also interesting from a fundamental point of view because, while current-induced DW motion has been observed experimentally well achieved [10–13], the underlaying theory of interaction between current and magnetization is still controversial. Some authors [14–17] claim that if the DW width is larger than a characteristic length, adiabatic conditions are fulfilled and, consequently, the spin of conduction electrons becomes fully polarized due to the local magnetization. The characteristic length to which the DW width has to be compared is, depending on the model, the spin diffusion length [18], the Larmor precession length [19], or the Fermi wavelength [20]. On the other hand, and motivated by the large discrepancies between experiments and the perfect adiabatic approach, other authors have argued that nonadiabatic corrections, related to the spatial mistraking of spins between conduction electrons and local magnetization, must be included for finite wall width [21–23]. Specifically, the relative importance of the adiabatic and the nonadiabatic spin torques in determining the DW motion is still the subject of much debate [6,21,22,24]. In a zero temperature analysis, He *et al.* [5] predicted that the degree of nonadiabaticity of the spin torque, described by the nonadiabatic dimensionless parameter ξ, strongly influences the combinations of fields and currents necessary to depin a DW initially trapped at a constriction. Since the exact value of the nonadiabatic parameter is difficult to compute from first principles, a study of the DW depinning from a notch as a function of j_a and H_e might help to ascertain the magnitude of ξ by direct comparison between experiments and simulations. Until today current-induced DW depinning from a notch has been observed only in a few experimental works [7–9]. Although there exist theoretical works focused on the analysis of the DW motion driven by H_e and/or j_a [16,17,20–22], thermal effects on the DW motion have not been addressed thoroughly. In particular, in the experiments done to explore the nonadiabatic limit at room temperature [7], the critical current for DW depinning is found to decrease linearly with increasing field, and the depinning time decreases exponentially with increasing both current and/or field. These observations cannot be described neglecting thermal fluctuations.

In this Letter, we firstly characterize the pinning potential generated by a constriction placed on a thin ferromagnetic wire by means of micromagnetic modeling. Then, the field and current-induced DW depinning at room temperature is analyzed by means of a one-dimensional model, and both perfect adiabatic ($\xi = 0$) and nonadiabatic ($\xi > 0$) cases are discussed.

We focus our attention on a thin Permalloy nanowire with $L_y \times L_z = 60 \times 3$ nm^2 cross section, where two notches (15 nm long, 6 nm wide) are symmetrically placed on both edges of the wire [see Fig. 1(a)]. A computational region of $L_x = 2$ μm in length, with the notch placed in the center, was discretized by means of a cubic computational mesh of $\Delta x = 3$ nm in size. The inset of Fig. 1(d) depicts the equilibrium state of the DW at rest. Its response to the action of magnetic fields ($B_e = \mu_0 H_e$) and/or electrical density currents (j_a) instantaneously applied along the wire axis (*x axis*) is evaluated by numerically solving the Landau-Lifshitz-Gilbert equation augmented by the spin-polarized adiabatic and the nonadiabatic torques as derived in [21]. Adiabatic and nonadiabatic torques are proportional to $b_J = \frac{j_a \mu_B P}{e M_s}$ and $c_J = \xi b_J$, respectively, where μ_B is the Bohr's magneton, $e < 0$ is the electric charge, P is the polarization factor, and ξ is the dimensionless nonadiabatic parameter. All numerical details of our micromagnetic code can be found in [25]. Typical Permalloy parameters are considered: saturation magneti-

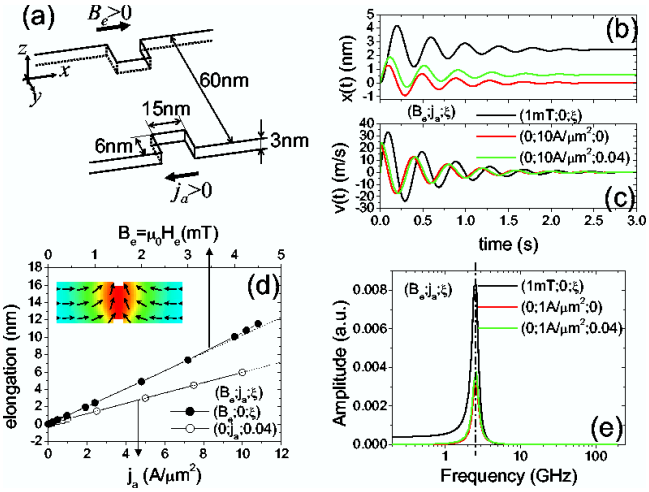

FIG. 1 (color online). Micromagnetic results in the pinned regime. (a) Schematic picture of the geometry dimensions considered. (b) and (c) depict the temporal evolution of the DW position and velocity for three different triplets $(B_e; j_a; \xi)$. (d) Terminal elongation of the DW as a function of the field $(B_e > 0; j_a = 0; \xi)$ (closed circles) and as a function of applied current $(B_e = 0; j_a > 0; \xi = 0.04)$ (open circles). The inset shows the initial equilibrium DW state. (e) Frequency spectrum corresponding to the characteristic DW oscillations around the notch.

zation $M_s = 860\,\mathrm{kA/m}$, exchange constant $A = 13$ pJ/m, damping $\alpha = 0.02$, and $P = 0.4$.

According to the sign criteria of Fig. 1(a), positive fields and/or currents (electrons flowing in positive x direction) exert an external force $F_e(B_e, j_a, \xi > 0)$ which pushes the DW to the right $(x > 0)$, where x indicates the DW position. For fields or currents below a given threshold ($B_e \leq 4.5$ mT, or $j_a \leq 10$ A/μm^2, with $\xi = 0.04$), the external force F_e is balanced by the restoring force F_p exerted by the notch, and the DW reaches a stationary position [$x(\infty)$, elongation] without leaving the notch. The temporal evolution of the DW position [$(x(t)$] and velocity [$v(t)$] for three different triplets $(B_e; j_a; \xi)$ are shown in Figs. 1(b) and 1(c). As observed, and contrary to the field-driven case, the adiabatic term of the current provides an initial DW velocity immediately after the application of the current [$v(0) = -\frac{b_J}{(1+\alpha^2)}$ [16]]. At zero field, the DW position returns to the initial state [$x(\infty) = 0$] after developing damped oscillations if perfect adiabatic conditions ($\xi = 0$) are assumed, whereas a positive elongation [$x(\infty) > 0$] from the center of the notch is found if nonadiabatic corrections ($\xi > 0$) are considered. The stationary DW elongation $x(\infty)$ as a function of $B_e > 0$ or $j_a > 0$ in the pinned regime is depicted in Fig. 1(c) for two different triplets: $F_e(B_e; 0; \xi)$ (closed symbols), and $F_e(0; j_a; \xi = 0.04)$ (open symbols). These micromagnetic results indicate that the DW elongation increases linearly with the external force in both cases up to the depinning threshold. Moreover, the computed spectrum from the Fourier transform of $v(t)$ is shown in Fig. 1(e), corresponding to the three cases depicted in Fig. 1(c). A single frequency peak of $f_{\mu M,N} = 2.59$ GHz is obtained, pointing out that the natural frequency is only related to the notch geometry and independent of the external force.

Based on the former micromagnetic analysis of the deterministic pinned regime, and in order to develop a further understanding of the thermally activated DW depinning from the notch, we adopt a well-established one-dimensional description which treats the DW as a rigid object inside a parabolic pinning potential. This model, which was originally introduced to describe the deterministic field-driven motion of DWs [26], has been recently extended to include spin torque [16,17,20–22] and thermal effects [25]. Assuming that the DW width remains constant independently of the field and the current ($\Delta_0 = 21.14$ nm [27]), and that the tilt angle between the magnetization with and the easy plane (xy plane) is very small [23], the linearized one-dimensional DW dynamics is determined by the Langevin equation (hereafter, 1DM)

$$m_w \frac{d^2x}{dt^2} = F_f + F_e + F_p(x) + F_t(t), \qquad (1)$$

where $m_w = \mu_0 L_y L_z \frac{2(1+\alpha^2)}{\gamma_0^2 (N_z - N_y)\Delta_0}$ is the effective DW mass, being N_y and N_z the transverse demagnetizing factors [28]. The terms on the right-hand side of Eq. (1) are the different contributions to the total force acting on the DW. The first one, $F_f = -\alpha[(\mu_0 L_y L_z)\frac{2M_s}{\gamma_0 \Delta_0} + \frac{K_N}{\gamma_0 (N_z - N_y) M_s}]v(t)$ is the friction force which is proportional to the DW velocity $v = \frac{dx}{dt}$ and the damping parameter α. The external driving force F_e has two contributions, one related to the external magnetic field $H_e = B_e/\mu_0$, and other relative to the applied current j_a, $F_e = F_H + F_j = (\mu_0 L_y L_z)(2M_s H_e - \frac{2M_s}{\gamma_0 \Delta_0} c_J)$. The third term on the right side $F_p(x)$ is the spatially dependent restoring force derived from the pinning potential $V_{\mathrm{pin}}(x)$ associated to the notch. Based on the micromagnetic characterization discussed above [see Figs. 1(d) and 1(e)], the pinning force $F_p(x) = -\frac{\partial V_{\mathrm{pin}}}{\partial x}$ can be described by means of a parabolic potential given by $V_{\mathrm{pin}}(x) = \frac{1}{2} K_N x^2$ if $|x| \leq L_N$, and $V_{\mathrm{pin}}(x) = 0$ if $|x| > L_N$. L_N represents the spatial extension of the pinning potential. The magnitude of the elastic constant of the notch K_N is straightforwardly inferred from the slope of linear behavior of the elongation as a function of the field-driven force of Fig. 1(d), which leads to $K_N = 1.27 \times 10^{-4}$ N/m. The natural frequency of the one-dimensional free harmonic oscillator is therefore analytically given by $f_N = \frac{1}{2\pi}\sqrt{\frac{K_N}{m_w}} = 2.59$ GHz, in good agreement with the micromagnetically computed value [see Fig. 1(e)]. The length of the pinning potential, $L_N = 16$ nm, was computed by fitting the depinning threshold field obtained micromagnetically. Lastly, thermal fluctuations are included in the formalism by means of a random

thermal force $F_t(t)$ which is a Gaussian-distributed stochastic noise process with zero mean value $\langle F_t(t)\rangle = 0$, and uncorrelated in time (white noise) $\langle F_t(t)F_t(t')\rangle = 2D_{1D}\delta(t-t')$. The factor D_{1D} represents the strength of the thermal force, which can be obtained from the fluctuation-dissipation theorem [25], $D_{1D} = \frac{m_w}{t_R} K_B T$ being $t_R^{-1} = \frac{\alpha}{1+\alpha^2}\gamma_0 M_s(N_z - N_y)$ the inverse of the time required by the system to reach $1/e$ of its terminal velocity. Equation (1) is numerically solved by means of a 4th-order Runge-Kutta scheme imposing an initial velocity of $v(0) = -\frac{b_J}{(1+\alpha^2)}$ [16,25], according to the micromagnetic simulations.

In Fig. 2, the averaged DW velocity over a temporal window of $t_w = 5$ μs is shown as a function of (B_e, j_a, ξ, T). Left and right pictures correspond, respectively, to the perfect adiabatic ($\xi = 0$) and nonadiabatic ($\xi = 0.04$) cases. Deterministic results for the temporal average DW velocity ($[v(t)]_{t_w} = \frac{1}{t_w}\int_0^{t_w} v(t)dt$) are shown in the top figures, whereas the bottom ones are computed at $T = 300$ K by first averaging over $n = 5000$ realizations [$\langle v\rangle_n(t) = \frac{1}{n}\sum_{i=1}^{n} v_i(t)$], and then averaging over the temporal window ($[\langle v\rangle_n(t)]_{t_w}$). At $T = 0$, the DW depinning only occurs if the current and the magnetic field are sufficiently large. On the contrary, at $T = 300$ K, the problem is no longer deterministic, and there is a non-null probability of DW depinning for driving forces smaller than the deterministic threshold. For $\xi = 0$, thermal fluctuations slightly reduce the deterministic depinning current up to $B_e \approx 2.1$ mT. For larger fields, an abrupt reduction of the critical depinning current is observed. This behavior is consistent with recent experimental observations for thick walls [8,9]. In the nonadiabatic case $\xi = 0.04$, thermal fluctuations significantly promote the DW depinning for $B_e > 0$, and the critical depinning current decreases linearly as the field is increased. Again, our results qualitatively explain the experimental measurements of [7], which were carried out in order to explore the nonadiabatic case for very thin walls. Once the DW leaves the notch, it depicts a fluctuating velocity with a mean value corresponding to the deterministic velocity along a free-defects wire, $v_D = \frac{1}{\alpha}(\gamma_0\Delta_0 H_e - c_J)$ [25].

In order to obtain further insight into the field and current-induced DW depinning, the probability distributions for the terminal DW velocity computed by our stochastic one-dimensional model (1DM) are shown in Fig. 3(a) for three different values of j_a under constant $B_e = 0.5$ mT = const. The parameters $\xi = 0.04$, $T = 300$ K, and $t_w = 5$ μs are fixed in the rest of the discussion. For $j_a = 1$ A/μm^2 the probability depicts a single peak Gaussian distribution for the DW velocity with zero mean value indicating that the DW remains pinned at the notch with 100% of probability. The width of the distribution is a consequence of thermal fluctuations. For sufficiently high currents ($j_a = 11$ A/μm^2), an analogous distribution is centered at a finite positive DW velocity, and therefore, the DW is in the viscous regime depinning from the notch with probability one. For intermediate

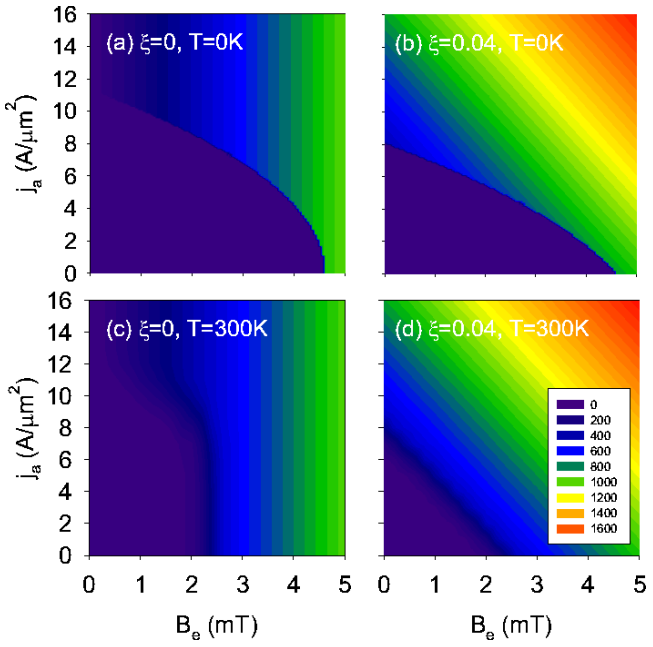

FIG. 2 (color online). Phase diagrams for averaged DW velocity (in m/s) as a function of (B_e, j_a, ξ, T) computed as described in the text. The values of ξ and T are indicated in the top left corner of each panel.

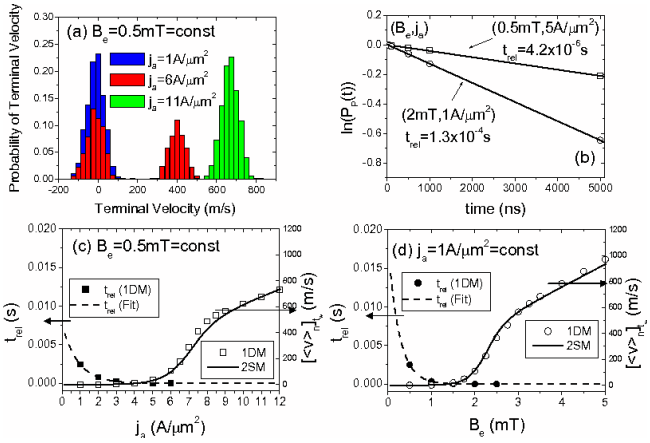

FIG. 3 (color online). (a) Histograms for the terminal velocity computed from the stochastic 1DM. B_e is fixed to 0.5 mT, and three values of j_a are shown. (b) Temporal evolution of the pinning probability $P_P(t)$ for two pairs of (B_e, j_a). In (c) and (d) the 1DM relaxation times $t_{\rm rel}$ (closed symbols), and the Arrhenius fits [30] (dashed lines) are depicted for (0.5 mT, j_a) and (B_e, 1 A/μm^2 respectively. The 1DM results for the averaged DW velocity $[\langle v\rangle_n]_{t_w}$ (open symbols) are compared with the 2SM (solid lines) predictions for both cases. Common parameters: $P = 0.4$, $\xi = 0.04$, $T = 300$ K, $t_w = 5$ μs, $n = 5000$.

currents ($j_a = 8$ A/μm^2), the histogram presents two different peaks: one centered at the zero DW velocity and another centered at a positive DW velocity value that corresponds to the free propagation DW velocity. In such a case, the DW depinning is thermally activated since the current is below than the deterministic depinning value. This analysis suggests that the depinning transition can be described in terms of a two states model (2SM) [29]. The master equation describing the temporal evolution for the probability that the DW remains pinned is $\frac{dP_P(t)}{dt} = -\omega_{PD} P_P(t)$, where P_P and $P_D = 1 - P_P$ represent the probability that the DW remains pinned and depinned, respectively, and $\omega_{PD} = t_{\mathrm{rel}}^{-1}$ is the probability per unit of time of observing a transition from the pinned state (P) to the depinned one (D). For a given t_w, the 2SM provides expressions for estimating the statistical averaged trajectory $\langle v \rangle_n(t)$, and the time averaged velocity $[\langle v \rangle_n(t)]_{t_w}$, if the relaxation time $t_{\mathrm{rel}}(B_e, j_a, \xi, T)$ is previously known: $\langle v \rangle_n(t) = v_D(1 - e^{t/t_{\mathrm{rel}}})$, and $[\langle v \rangle_n(t)]_{t_w} = v_D[1 - \frac{t_{\mathrm{rel}}}{t_w}(1 - e^{-t_w/t_{\mathrm{rel}}})]$. The $t_{\mathrm{rel}}(B_e, j_a, \xi, T)$ can be deduced by fitting the 1DM results to the 2SM solution ($P_P(t) = e^{-\omega_{PD} t}$). An example of this fitting is shown in Figs. 3(b) for two pairs of (B_e, j_a). The same fitting procedure was carried out for several values of (B_e, j_a), and it was confirmed that 1DM results for t_{rel} [see closed symbols in both Fig. 3(c) and 3(d)] can be successfully fitted to the Arrhenius empirical law $t_{\mathrm{rel}} = \tau_0 e^{E_b/K_B T}$, where τ_0 represents the characteristic time constant, and $E_b(B_e, j_a)$ is the energy barrier between P and D states [30]. Introducing the expression of t_{rel} in the 2SM equation for $[\langle v \rangle_n(t)]_{t_w}$ (solid lines), we can compare it with the 1DM results (open symbols) in Figs. 3(c) and 3(d). A good agreement is found in both cases, showing that the 2SM describes accurately the stochastic nature of these processes.

In summary, we have presented a stochastic one-dimensional model which allows to describe thermal effects on the DW depinning as a function of both the external field and the applied current. This rigid model cannot capture complex dynamical processes like the possible DW distortion or spin waves excitations. It can neither account for the temperature increase due to the Joule heating introduced by the electrical current, because the Langevin formalism is only valid for a fixed temperature of the thermal bath. However, the stochastic one-dimensional model appears to describe well the essential physical mechanisms responsible for the thermal dependence of the DW depinning. On one hand, the 1DM qualitatively explains the linear decreasing of the critical current with increasing the field observed in experiments done to explore the nonadiabatic regime [7] in thin ferrromagnetic walls. The exponential decrease of the depinning time with increasing both current and/or field observed in [7] is also explained by the 1DM. On the other hand, the stochastic 1DM is also consistent with the depinning current dependence on the field addressed in very recent experiments for thick walls [8,9], where the adiabatic conditions are assumed to dominate the DW depinning. Thus, once we characterized the details of the pinning potential for each particular notch, our method allows us to characterize the stochastic behavior of the DW depinning process, which, on one hand, has to be taken into account for future spintronic applications and, on the other, constitutes a useful framework to obtain information on the nonadiabaticity degree of the spin torque by direct comparison with experiments.

This work was partially supported by Projects No. MAT2005-04827 from the Spanish government, and No. SA063A05 from Junta de Castilla y Leon.

[1] D. A. Allwood *et al.*, Science **309**, 1688 (2005).
[2] S. S. P. Parkin, U.S. Patent No. 6834005 2004.
[3] L. Thomas *et al.*, Appl. Phys. Lett. **87**, 262501 (2005).
[4] A. Himeno *et al.*, J. Appl. Phys. **99**, 08G304 (2006).
[5] J. He *et al.*, J. Appl. Phys. **98**, 016108 (2005).
[6] L. Thomas *et al.*, Nature (London) **443**, 197 (2006).
[7] D. Ravelosona *et al.*, Phys. Rev. Lett. **95**, 117203 (2005).
[8] M. Hayashi *et al.*, Phys. Rev. Lett. **97**, 207205 (2006).
[9] P. Dagras *et al.*, J. Phys. D: Appl. Phys. **40**, 1247 (2007).
[10] G. S. D. Beach *et al.*, Phys. Rev. Lett. **97**, 057203 (2006).
[11] M. Klaui *et al.*, Appl. Phys. Lett. **87**, 102509 (2005).
[12] M. Laufenberg *et al.*, Appl. Phys. Lett. **88**, 052507 (2006).
[13] J. Grollier *et al.*, Appl. Phys. Lett. **83**, 509 (2003).
[14] L. Berger, J. Appl. Phys. **49**, 2156 (1978).
[15] Ya. B. Bazaliy *et al.*, Phys. Rev. B **57**, R3213 (1998).
[16] Z. Li *et al.*, Phys. Rev. B **70**, 024417 (2004); Z. Li *et al.*, Phys. Rev. Lett. **92**, 207203 (2004).
[17] A. Thiaville *et al.*, J. Appl. Phys. **95**, 7049 (2004).
[18] S. Zhang *et al.*, Phys. Rev. Lett. **88**, 236601 (2002).
[19] X. Waintal *et al.*, Europhys. Lett. **65**, 427 (2004).
[20] G. Tatara *et al.*, Phys. Rev. Lett. **92**, 086601 (2004).
[21] S. Zhang *et al.*, Phys. Rev. Lett. **93**, 127204 (2004).
[22] A. Thiaville *et al.*, Europhys. Lett. **69**, 990 (2005).
[23] Z. Li *et al.*, J. Appl. Phys. **99**, 08Q702 (2006).
[24] J. He *et al.*, J. Appl. Phys. **97**, 10C703 (2005).
[25] E. Martinez *et al.*, Phys. Rev. B **75**, 174409 (2007).
[26] N. L. Schryer and L. R. Walker, J. Appl. Phys. **45**, 5406 (1974).
[27] The DW width is computed according to Thiele's definition [A. A. Thiele, Phys. Rev. Lett. **30**, 230 (1973)]. A value of $\Delta_0 = 21.14$ nm was obtained in the absence of field and current. Micromagnetic simulations indicate that the relative change of the DW width with respect to the static case remains smaller than 0.05% in the whole pinned range.
[28] A. Aharoni, J. Appl. Phys. **83**, 3432 (1998).
[29] G. Bertotti, *Hysteresis in Magnetism* (Academic, San Diego, 1998).
[30] For the two particular cases presented in Figs. 3(c) and 3(d), we obtain $\tau_0 = 7.67$ ms and $E_b/K_B T = -1.13 j_a$[A/μm^2] for (0.5 mT, j_a, 0.04, 300 K), and $\tau_0 = 0.17$ ms and $E_b/K_B T = -3.88 B_e$[mT] for (B_e, 1 A/μm^2, 0.04, 300 K), respectively.